

Short communication

Cyclic voltammetry of $\text{LiCr}_{0.15}\text{Mn}_{1.85}\text{O}_4$ in an aqueous LiNO_3 solution

Nikola Cvjeticanin^a, Ivana Stojkovic^a, Miodrag Mitric^b, Slavko Mentus^{a,*}

^a Faculty of Physical Chemistry, Belgrade University, Studentski trg 12-16, P.O. Box 137, 11001 Belgrade, Serbia

^b The Vinča Institute of Nuclear Sciences, Laboratory for Theoretical and Condensed Matter Physics, P.O. Box 522, 11001 Belgrade, Serbia

Available online 26 June 2007

Abstract

Cyclic voltammetry (CV) of $\text{LiCr}_{0.15}\text{Mn}_{1.85}\text{O}_4$, synthesized by rapid glycine-nitrate method (GNM), was performed in a saturated aqueous LiNO_3 ($\sim 9\text{ M}$) solution. At rather high polarization rate of 10 mV s^{-1} two well separated characteristic pairs of redox peaks can be clearly observed, which is not entirely the case for LiMn_2O_4 synthesized in the same way. At a reduced scan rate of 1 mV s^{-1} , the shape and position of redox peaks evidence that deintercalation/intercalation of Li^+ ion is highly reversible and much faster than in the case of organic electrolytes. Faster “CV response” of $\text{LiCr}_{0.15}\text{Mn}_{1.85}\text{O}_4$ is in correlation with higher capacity retention (93%) in comparison to LiMn_2O_4 (88%), registered after 50 charging/discharging cycles in organic electrolyte solution (1 M LiClO_4 in propylene carbonate).

© 2007 Elsevier B.V. All rights reserved.

Keywords: Cyclic voltammetry; Aqueous LiNO_3 solution; Cathodic materials; $\text{LiCr}_{0.15}\text{Mn}_{1.85}\text{O}_4$; LiMn_2O_4 ; Glycine-nitrate method

1. Introduction

LiMn_2O_4 spinel is very promising, environmentally friendly, cathodic material for lithium batteries, but its disadvantage is poor cycling performance caused by several proposed mechanisms: the dissolution of Mn, the position exchange between Li and Mn during discharge, the aggressiveness toward organic electrolyte, etc. [1]. Shin and Manthiram [2,3] published that lattice parameter difference Δa between the two cubic phases formed in the two-phase region [4] plays the main role in the capacity fade. Δa can cause instantaneous volume change in the 4 V two-phase region which can be considered as analogous to volume change occurring during Jahn-Teller distortion in the 3 V region. Partial Mn substitution by other metals ($M = \text{Zn, Ni, Al, Cr, etc.}$) decreases Δa and leads to a better capacity retention. Δa is especially low when degree of substitution is such that average Mn oxidation state is beyond 3.58. In that case the change of lithium content develops only small or no microstrain and thus there is no hindrance to lithium diffusion in the spinel lattice [2,3]. Cr^{3+} is among the cations whose substitu-

tion for manganese gives the most robust spinels [5–9]. The reason for such behavior may be the fact that Cr^{3+} increases Li–O–Mn bond covalency more than other substitutional cations [1].

Commercial lithium-ion batteries use only organic electrolytes. Aqueous lithium-ion cells did not experience commercial use, primarily because there is no suitable anode material compatible with water solutions. Rocking-chair battery using LiMn_2O_4 as both the anode and the cathode, in an aqueous solution, is not feasible. $\text{LiMn}_2\text{O}_4/\text{LiNO}_3, \text{Zn}^{2+}/\text{Zn}$ was the only battery reported to use Li-intercalate and aqueous electrolyte solution [10]. Li and Dahn [11] reported that nevertheless rechargeable lithium-ion cells with aqueous electrolytes (LiOH or LiNO_3) are feasible, if LiMn_2O_4 is used as anode and VO_2 or $\gamma\text{-Li}_{0.36}\text{MnO}_2$ as cathode. This cell type produces the voltage of 1.5 V. [11]. Recently, LiMn_2O_4 , having spinel structure as a positive electrode, was combined with an activated carbon negative electrode to obtain a battery which uses a Li_2SO_4 aqueous solution as the electrolyte [12].

According to our knowledge, the reports related to the $\text{LiCr}_x\text{Mn}_{2-x}\text{O}_4$ spinels published thus far, do not concern their intercalation/deintercalation behavior of in aqueous solutions. In this work we compared the cyclovoltammograms of $\text{LiCr}_{0.15}\text{Mn}_{1.85}\text{O}_4$ and LiMn_2O_4 , both synthesized by rapid

* Corresponding author.

E-mail address: slavko@ffh.bg.ac.yu (S. Mentus).

GNM, using saturated aqueous solution of LiNO_3 as electrolyte. The constant current charging/discharging performances were tested in 1 M LiClO_4 in PC. The crystallographic structure and morphology of both materials were examined too.

2. Experimental

2.1. Sample preparation

Glycine-nitrate method (GNM) was applied for the synthesis of $\text{LiCr}_{0.15}\text{Mn}_{1.85}\text{O}_4$ and LiMn_2O_4 spinels. Details of experimental procedure are described in our previous papers [13] Aqueous solutions of LiNO_3 , $\text{Cr}(\text{NO}_3)_3 \cdot 9\text{H}_2\text{O}$, and $\text{Mn}(\text{NO}_3)_2 \cdot 4\text{H}_2\text{O}$ were mixed in appropriate volume ratios in order to obtain desired stoichiometry, and solid glycine was added and dissolved to obtain precursor solution. The precursor solutions was placed in a glass beaker and heated in an oven to evaporate water, and then the heating was continued until spontaneous ignition occurred. The ash, resulted from the combustion, was heated at 800°C for 4 h.

2.2. Sample morphology and structure

The samples obtained in powdery form were examined by X-ray powder diffraction, scanning electron microscopy, cyclic voltammetry (CV) and galvanostatic cycling.

The XRPD experiments were performed with Philips 1050 diffractometer using $\text{CuK}\alpha_{1,2}$ radiation. The $15\text{--}70^\circ$ 2θ angles were used because most intensive reflections of lithium manganese spinels appear in this range. Exposition time was 2 s and step was 0.05° .

The microphotographs for the purposes of this study were recorded on JEOL JSM-6460 LV.

For electrochemical measurements, working electrode was made from intercalate powder, carbon black and PVDF mixed in a weight ratio 85:10:5. The slurry, prepared by addition of this mixture in *N*-methyl-2-pyrrolidone, was treated for 30–60 min in an ultrasonic bath, and then deposited on a platinum foil ($\sim 2\text{ cm}^2$). The electrode was dried under vacuum at 120°C over night before it was transferred into the glove box. The mass of active cathode material amounted to between 2 and 4 mg cm^{-2} . CV experiments were carried out in the saturated ($\sim 9\text{ M}$) aqueous LiNO_3 solution by using EG&G PAR Potentiostat/Galvanostat Model 273. Wide platinum foil was used as a counter electrode. CVs were recorded from 0 to 1.5 V versus saturated calomel electrode (SCE), used as the reference electrode. Galvanostatic charging/discharging experiments between cutoff voltage of 4.3 and 3.1 V were performed in an organic electrolyte. Two-electrode cell placed in a dry-argon box was used, in which lithium foil served as the counter electrode. Constant current source was a home made, software controlled current stabilizer. A 1 M LiClO_4 (Lithium corporation of America) in PC (Fluka) was used as electrolyte. PC was purified by distillation under reduced pressure, and the middle 2/3 fraction was used. Before dissolving, LiClO_4 was dried over night at $130\text{--}140^\circ\text{C}$ under reduced pressure.

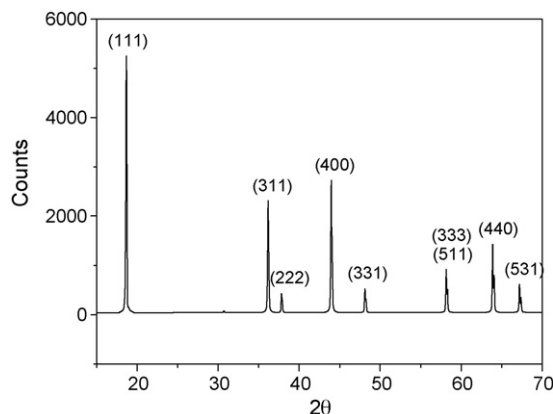


Fig. 1. The X-ray diffractogram of $\text{LiCr}_{0.15}\text{Mn}_{1.85}\text{O}_4$ spinel obtained by GNM.

3. Results and discussion

3.1. Structure and morphology

The XRPD patterns of the investigated materials, shown in Figs. 1 and 2, correspond to a pure spinel phase. The lattice parameters were determined to be $a=8.234\text{ \AA}$ for $\text{LiCr}_{0.15}\text{Mn}_{1.85}\text{O}_4$ and $a=8.241\text{ \AA}$ for LiMn_2O_4 . These values agree very well with the ones published elsewhere for this kind of spinels [5,7,14,15]. The reduction in $\text{LiCr}_{0.15}\text{Mn}_{1.85}\text{O}_4$ lattice parameter is a consequence of increased manganese oxidation state, as a result of Cr^{3+} for Mn^{3+} substitution.

SEM microphotographs of $\text{LiCr}_{0.15}\text{Mn}_{1.85}\text{O}_4$ and LiMn_2O_4 powders are shown in Fig. 3. The average particle diameter is below 500 nm for both spinels. The particles are polyhedral in shape, and $\text{LiCr}_{0.15}\text{Mn}_{1.85}\text{O}_4$ show less degree of sintering than LiMn_2O_4 .

3.2. Electrochemical performance

CV in a saturated aqueous LiNO_3 solution, performed at relatively high polarization rate of 10 mV s^{-1} , Fig. 4a, reveals two pairs of redox peaks for $\text{LiCr}_{0.15}\text{Mn}_{1.85}\text{O}_4$ which is typical of unsubstituted and low substituted lithium manganese spinels. The anodic peaks are centered at 1.01 and 1.15 V, while

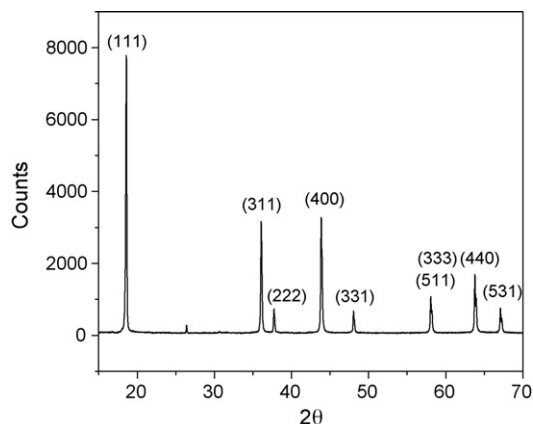


Fig. 2. The X-ray diffractogram of LiMn_2O_4 spinel obtained by GNM.

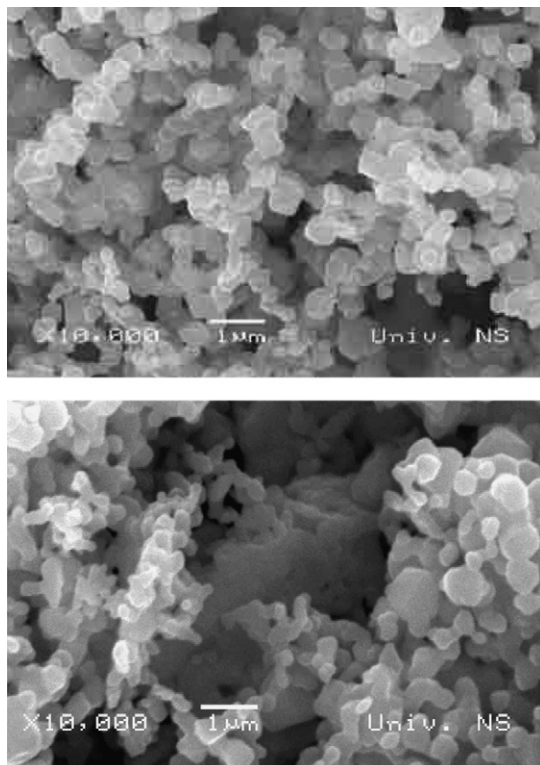


Fig. 3. SEM micrographs of $\text{LiCr}_{0.15}\text{Mn}_{1.85}\text{O}_4$ (up) and LiMn_2O_4 (down). The length of the white bar is $1\ \mu\text{m}$.

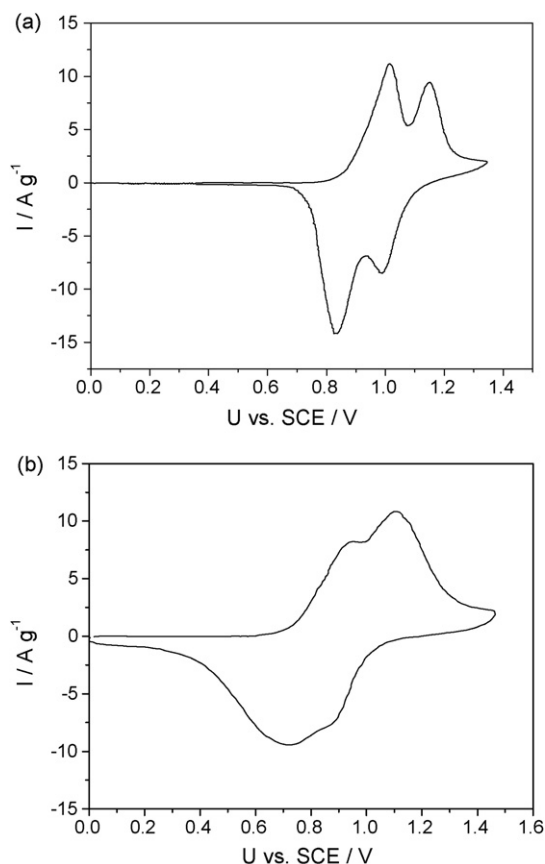


Fig. 4. Cyclic voltammograms in LiNO_3 water solution: (a) $\text{LiCr}_{0.15}\text{Mn}_{1.85}\text{O}_4$ and (b) LiMn_2O_4 . Scan rate $10\ \text{mV s}^{-1}$.

corresponding cathodic peaks are centered at 0.83 and 0.99 V versus SCE. The deintercalation/intercalation of LiMn_2O_4 at $10\ \text{mV s}^{-1}$ does not show such well resolved peaks Fig. 4b. This fact implies that chromium doped spinels have faster “response” than undoped one. At a reduced scan rate of $1\ \text{mV s}^{-1}$ the CVs with fully resolved redox peaks were obtained for both spinels (Fig. 5a and b). They display the same shape as CVs recorded in organic electrolytes, at one order of magnitude lower scan rates [5,9,14,16,17]. In the case of $\text{LiCr}_{0.15}\text{Mn}_{1.85}\text{O}_4$, the height of the second pair of redox peaks, Fig. 5a, is lower than for the first pair while opposite conclusion is valid for LiMn_2O_4 , Fig. 5b. The presence of Cr^{3+} reduces the amount of manganese ions which could be oxidized and reduced during extraction and insertion, respectively, of Li^+ ions. This reduces both the charge/discharge capacity of doped spinel in high potential region, and the intensity of second pair of redox peaks.

At a polarization rate of $1\ \text{mV s}^{-1}$ the anodic peaks of $\text{LiCr}_{0.15}\text{Mn}_{1.85}\text{O}_4$ are centered at 0.90 and 1.04 V, while the corresponding cathodic ones are centered at 0.83 and 0.97 V versus SCE, Fig. 5a. The separation of anodic and cathodic peaks is the same or even less pronounced than the one we recorded previously for the same material in $1\ \text{M LiClO}_4$ in PC at $50\ \mu\text{V s}^{-1}$ [13]. This evidences a high degree of reversibility of $\text{LiCr}_{0.15}\text{Mn}_{1.85}\text{O}_4$ electrode in water solution. The anodic and cathodic peaks for LiMn_2O_4 are centered at 0.92 V, 1.05 V and 0.83 V, 0.95 V vs. SCE, respectively. In this case the separa-

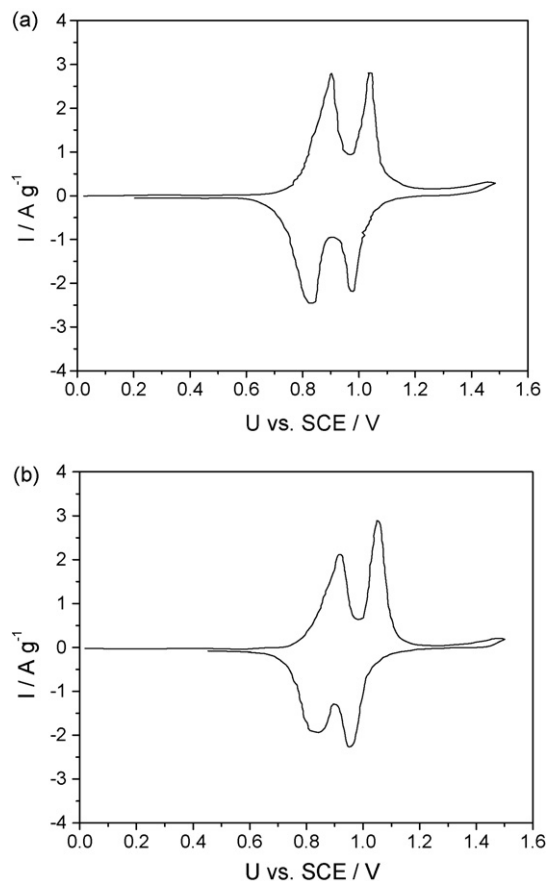


Fig. 5. Cyclic voltammograms in LiNO_3 water solution: (a) $\text{LiCr}_{0.15}\text{Mn}_{1.85}\text{O}_4$ and (b) LiMn_2O_4 . Scan rate $1\ \text{mV s}^{-1}$.

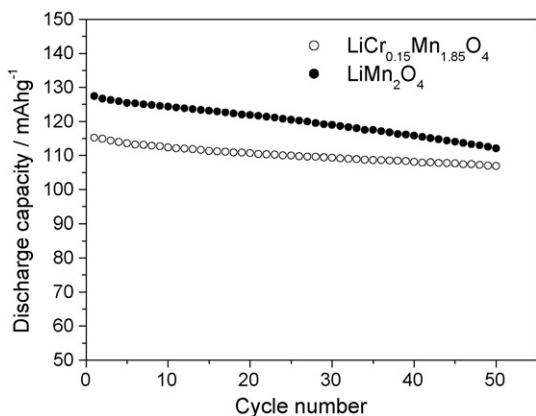


Fig. 6. The discharge capacity of $\text{LiCr}_{0.15}\text{Mn}_{1.85}\text{O}_4$ (○) and LiMn_2O_4 (●) in 1 M LiClO_4 in PC at a rate of 50 mAh g^{-1} .

ration of appropriate peaks is somewhat larger, i.e., the degree of reversibility is slightly lower. Zhang et al. [17] investigating the shape of CVs of lithium intercalation by mathematical modeling, have shown that shape of CVs like that given in Fig. 5., corresponds to a case when interfacial reaction kinetics is fast, and whole intercalation process is controlled by the Li^+ diffusion in the solid host. This points out that very high rate of intercalation/deintercalation in water solution, especially in the case of $\text{LiCr}_{0.15}\text{Mn}_{1.85}\text{O}_4$, is thanks to both the absence of high-resistant layer (otherwise always present at the organic electrolyte/cathode material interface) and the high concentration of Li^+ ions in water solution.

In order to correlate CV experiments in aqueous solution to charge/discharge behavior in real batteries we performed constant current charge/discharge cycling of our materials in organic electrolyte, 1 M LiClO_4 solution in PC. These examinations evidenced (Fig. 6.) lower value of initial discharge capacity of $\text{LiCr}_{0.15}\text{Mn}_{1.85}\text{O}_4$ (115 mAh g^{-1}) in comparison to LiMn_2O_4 (127 mAh g^{-1}). This may be treated as an expected consequence of the reduced concentration of Mn^{3+} ions in this Cr^{3+} doped spinel. After 50 cycles the discharge capacity of $\text{LiCr}_{0.15}\text{Mn}_{1.85}\text{O}_4$ decreases to 93% of its initial value, while capacity retention for LiMn_2O_4 becomes 88%, Fig. 6. We may conclude that chromium doped spinel, characteristic of better resolved redox peaks in CV's (Figs. 4a and 5a), exhibits also lower capacity fading during galvanostatic cycling (Fig. 6). This creates an opportunity to predict long term cycling behavior of potential cathodic and anodic materials by fast CV experiments in water solutions without using dry box. This method is unfortunately limited to such materials only which intercalate and deintercalate lithium within a voltage window narrower than the one of water electrolysis.

Capacity retention of LiMn_2O_4 synthesized by GNM should also be considered as very good. LiMn_2O_4 obtained by solid

state reaction, at similar or lower charging/discharging rates, retains only 60% of its initial capacity [2,3,5]. This recommends GNM as very promising method of simple and rapid synthesis of doped and undoped spinel compounds.

4. Conclusions

GNM is rapid, simple and low cost synthetic route which may be used for synthesis of different, both undoped and doped, kinds of spinel compounds displaying advantageous initial capacity and cycling life than the ones obtained by solid state reaction. Using this method, LiMn_2O_4 spinel was synthesized in which Mn was partially replaced by Cr, and this material, used as a cathode material of a Li-ion battery, displayed more stable cycling life than the original spinel synthesized in the same way.

CV in aqueous solution of LiNO_3 may be used as a fast and simple method to test cathodic and anodic materials and to predict their long-term constant current cycling behavior.

Acknowledgements

This work has been partially supported by the Ministry of Science and Environmental Protection of Republic Serbia (Project No. 142047).

References

- [1] M.C. Tucker, J.A. Reimer, E.J. Cairns, J. Electrochem. Soc. 149 (2002) A1409.
- [2] Y. Shin, A. Manthiram, Electrochem. Solid-State Lett. 5 (3) (2002) A55.
- [3] Y. Shin, A. Manthiram, J. Electrochem. Soc. 151 (2) (2004) A204.
- [4] W. Liu, K. Kowal, G.C. Farrington, J. Electrochem. Soc. 145 (2) (1998) 459.
- [5] M.C. Tucker, J.A. Reimer, E.J. Cairns, J. Electrochem. Soc. 149 (5) (2002) A574.
- [6] C. Sigala, D. Guyomard, A. Verbaere, Y. Piffard, M. Tournoux, Solid State Ionics 81 (1995) 167.
- [7] L. Guohua, H. Ikuta, T. Uchida, M. Wakihara, J. Electrochem. Soc. 145 (1) (1996) 178.
- [8] C.-H. Lu, Y. Lin, H.-C. Wang, J. Mater. Sci. Lett. 22 (2003) 615.
- [9] Y.-P. Fu, Y.-H. Su, C.-H. Lin, Solid State Ionics 166 (2004) 137.
- [10] W. Pei, Y. Hui, Y. Huaquan, J. Power Sources 63 (1996) 275.
- [11] W. Li, J.R. Dahn, J. Electrochem. Soc. 142 (6) (1995) 1742.
- [12] Y. Wang, Y. Xia, Electrochem. Commun. 7 (2005) 1138.
- [13] I. Stojkovic, A. Hosseinmardi, D. Jugovic, M. Mitric, N. Cvjeticanin, Solid State Ionics 177 (2006) 847.
- [14] W. Liu, G.C. Farrington, E. Chaput, B. Dunn, J. Electrochem. Soc. 143 (3) (1996) 874.
- [15] P. Arora, B.N. Popov, R.E. White, J. Electrochem. Soc. 145 (3) (1998) 807.
- [16] B.-J. Hwang, Y.-W. Tsai, R. Santhanam, S.-K. Hu, H.-S. Sheu, J. Power Sources 119–121 (2003) 727.
- [17] D. Zhang, B. Popov, R. White, J. Electrochem. Soc. 147 (3) (2000) 831.